

A Green Route to Novel Hyperbranched Electrolyte Interlayer for Nonfullerene Polymer Solar Cells with Over 11% Efficiency

Dan Zhou ^{† [a], [b]}, Sixing Xiong ^{† [c]}, Lie Chen ^{* [b]}, Xiaofang Cheng ^[b], Haitao Xu ^[a],
Yinhua Zhou ^{* [c]}, Feng Liu ^{* [d]} and Yiwang Chen ^{* [b]}

^aKey Laboratory of Jiangxi Province for Persistent Pollutants Control and Resources Recycle, Nanchang Hangkong University, 696 Fenghe Avenue, Nanchang 330063, China

^bCollege of Chemistry, Nanchang University, 999 Xuefu Avenue, Nanchang 330031, China

^cWuhan National Laboratory for Optoelectronics, Huazhong University of Science and Technology, 1037 Luoyu Road, Wuhan 430074, China

^dDepartment of Physics and Astronomy, Shanghai Jiaotong University, 800 Dongchuan Road, Shanghai 200240, China

Corresponding author. Tel.: +86 791 83968703; fax: +86 791 83969561. E-mail: ywchen@ncu.edu.cn (Y. Chen), chenlie@ncu.edu.cn (L. Chen), yh_zhou@hust.edu.cn (Y. Zhou), fengliu82@sjtu.edu.cn (F. Liu).

Author contributions. D. Zhou and S. Xiong contributed equally to this work.

Materials and Methods

General Information.

EXPERIMENTAL SECTION

Materials:

Tetraethylene pentamine, 1,4-Butanesultone and hydride sodium were purchased from Aldrich or TCI. Ag (99.99 %) and MoO₃ (99.99 %) were purchased from Alfa Aesar. ITIC (99 %) and PBDB-T(99 %) were purchased from Solarmer Materials, Inc. and used without further purification. Indium-tin oxide (ITO) glass was purchased from Delta Technologies Limited.

Device Fabrication

The PBDB-T/ITIC devices were manufactured with the structure of Glass/ITO/ZnO/PNSO₃Na/active layer/MoO₃/Ag. The conductive ITO substrates were cleaned with ultrasonication in acetone, detergent, deionized water, and isopropanol for three times, respectively. After the ITO substrates were dried by nitrogen purging and treated the surface with UV ozone for 15 min. The ZnO precursor solution was spin-coated at 4000 rpm/min on the surface of the ITO-glass substrates and annealed at 225 °C for 1 h in air. The hyperbranched small molecule electrolyte (SME) PNSO₃Na (1.0 mg/mL dissolved in methanol) solution was spin-coated onto ZnO at 4000 r/min for 1 min under air atmosphere. The active layer PBDB-T/ITIC (1:1, w/w), a blend solution of 7 mg of PBDB-T and 7 mg of ITIC dissolved in 0.95 mL dichlorobenzene and 0.05 mL 1,8-diiodooctane solution with a total concentration of 14 mg mL⁻¹, the solution was spin-casted at 1100 rpm for 60 s. And then the film was annealed at 140 °C for 1 min in a nitrogen-atmosphere glove box. Subsequently, the anode buffer layer MoO₃ (7 nm) and Ag (90 nm) electrode were deposited on the active layer by thermal evaporation under a vacuum chamber to accomplish the device fabrication. The effective area of each cell was 0.041 cm². The current–voltage (*J–V*) curve was measured by a Keithley 2400 Source Meter under simulated solar light (100 mW/cm², AM 1.5 G, Abet Solar Simulator Sun 2000).

Synthesis

The detailed synthetic procedure of the target hyperbranched small molecule electrolyte (SME) PNSO₃Na is displayed in **Scheme S1**. The hyperbranched SME PNSO₃Na is first prepared by a green-route one-step simple reaction between tetraethylene pentamine and 1,4-butanedisulfone with nonhalogen solvent and purified by easy dialysis. The chemical structure of the PNSO₃Na was confirmed by ¹H nuclear magnetic resonance spectra (¹H NMR) (**Fig. S1**).

Synthesis of PNSO₃Na

Under the protection of nitrogen, tetraethylene pentamine (1.89 g, 0.01 mol) and dried THF (60 mL) were added to 250 mL round bottom flask. The reaction mixture was cooled to 0 °C in an ice bath, then NaH 3.0 g (60%) was slowly added to the solution

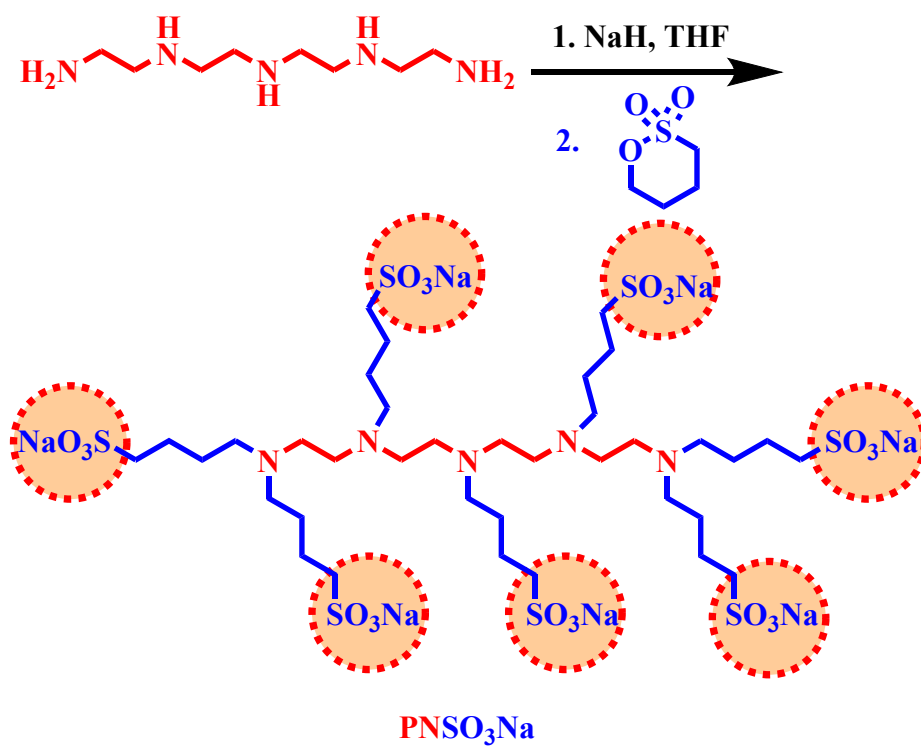
and the mixture was stirred at 0 °C for 0.5 h, the solution was gradually warmed to room temperature and stirred overnight. 1,4-Butanesultone (13.6 g, 0.1mol) was added to the reaction mixture, and the reaction solution was refluxed at 78 °C overnight. After cooling to room temperature, the reaction solution was dissolved in methanol solution and purified by a dialysis bag (pore diameter: 1000), dried under vacuum yield light yellow solid (71%). ¹H NMR (400 MHz, CD₃OD-*d*₄), (ppm): 3.459-3.320 (t, 14H, *J*=2.78 Hz), 3.245-2.510 (m, 30H), 1.887-1.765 (m,14H), 1.748-1.612 (m,14H).

Characterizations

The nuclear magnetic resonance (NMR) spectra were measured on a Bruker ARX 400 NMR spectrometer with deuterated methanol as the solvent and with tetramethylsilane ($\delta=0$) as the internal standard. Ultraviolet–visible (UV) spectra and optical transmittance spectra of the samples were recorded on a Hitachi UV-3010 spectrophotometer. Fluorescence measurement was carried out on the Edinburgh instruments FLS980. XPS studies were performed on a Thermo-VG Scientific ESCALAB 250 photoelectron spectrometer using a monochromated AlK α (1,486.6 eV) X-ray source. All recorded peaks were corrected for electrostatic effects by setting the C–C component of the C 1s peak to 284.8 eV. The base pressure in the XPS analysis chamber was 2×10^{-9} mbar. The work functions of the modified cathode were investigated using a Kelvin probe (KP 6500 Digital Kelvin probe, McAllister Technical Services. Co.,Ltd.), which can detect the contact potential difference (VCPD) and the work function difference ($\Delta\Phi=e\times\text{VCPD}$), where *e* is the electron charge between the probe and the sample. The Kelvin probe microscopy (KPM) shown in the figures are obtained by subtracting the pristine values from the work function of Au probe tip, which is 5.1 eV. The total 225 points are measured over the scan area of 1.5 mm \times 1.5 mm for each sample. The work function value was the average value of 144 points. The UPS measurements were carried out in a Thermo-VG Scientific ESCALAB 250 using a He I (21.22 eV) discharge lamp. A bias of -8.0 V was applied to the samples for separation of the sample and the secondary edge for the analyzer. The HOMO energies are determined by

$$-HOMO = hv - (E_{\text{cutoff}} - E_{\text{onset}})$$

Where hv is the incident photon energy, $hv = 21.22$ eV. E_{cutoff} is defined as the high binding energy cutoff; E_{onset} is the HOMO energy onset, generally referred to as the low binding energy onset. Atomic force microscopic (AFM) images were measured on a nanoscope III A (Digital Instruments) scanning probe microscope using the tapping mode. TEM images were recorded using a JEOL-2100F transmission electron microscope and an internal charge-coupled device (CCD) camera. Current-voltage (J - V) characteristics were recorded using Keithley 2400 Source Meter in the dark under 100 mW/cm² simulated AM 1.5 G irradiation (Abet Solar Simulator Sun 2000). The concentration and rotate speed of the small molecule electrolyte **PNSO₃Na** in UPS and KPM characterizations are consistent with those in the solar cell devices, the concentration of the hyperbranched small molecule electrolyte **PNSO₃Na** is 1.0 mg/mL, and the rotate speed is 4000 r/min. Grazing incidence X-ray scattering characterization of the thin films was performed at the Advanced Light Source on beamline 7.3.3, Lawrence Berkeley National Lab (LBNL).



Scheme S1. Synthesis route of hyperbranched small molecule electrolyte PNSO_3Na .

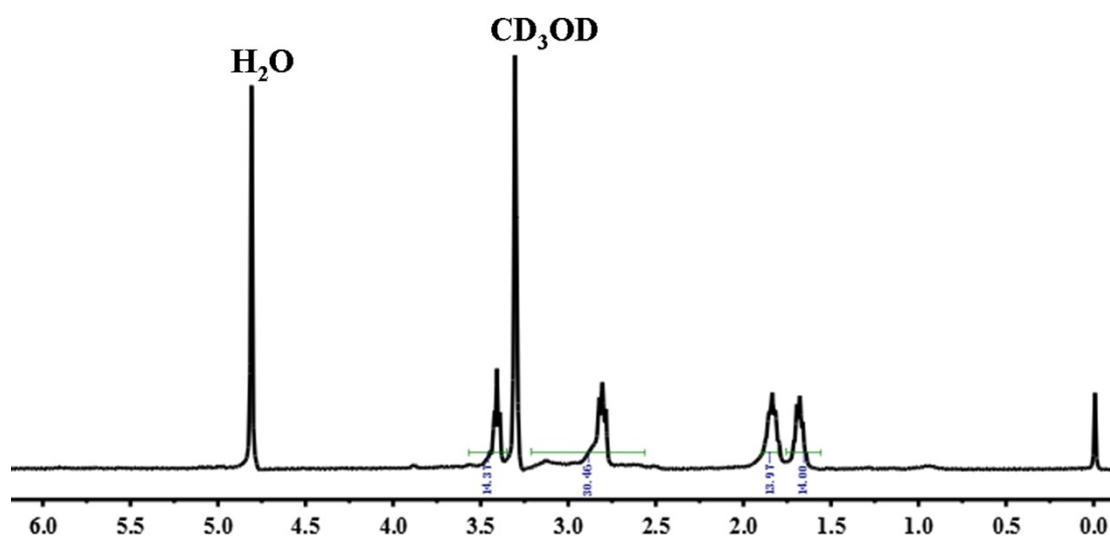


Fig. S1 The ¹H NMR spectrum of PNSO₃Na recorded in deuterated methanol solution.

To explore the interfacial interactions between **PNSO₃Na** and ZnO, X-ray photoelectron spectroscopy (XPS) of ZnO and ZnO/**PNSO₃Na** has been carried out (Fig. S2a, ESI†). The high resolution Na 1s XPS spectra of ZnO and ZnO/**PNSO₃Na** are shown in Fig. S2b (ESI†). There are no Na 1s signal peaks in the pure ZnO film, while a peak at 1071.25 eV can be clearly observed in the ZnO/**PNSO₃Na** film, which corresponds to the sodium atoms in the branched chain sodium sulfonate. Fig. S2c (ESI†) contains the high resolution O 1s XPS spectra of ZnO and ZnO/**PNSO₃Na** and two peaks at 532.00 eV and 530.40 eV have been detected for the bare ZnO. Meanwhile, the O 1s peaks of ZnO/**PNSO₃Na** have been shifted to 531.79 eV and 529.96 eV, respectively. Compared to the bare ZnO, the O 1s peaks of ZnO/**PNSO₃Na** have been shifted toward a lower binding energy, which suggests that a strong interfacial interaction exists at the ZnO and **PNSO₃Na** interface. S 2p high resolution spectra of ZnO and **PNSO₃Na** modified ZnO are shown in Fig. S2d (ESI†), no signals are discovered in the bare ZnO and a strong peak at 168.3 eV, corresponding to the sulfur atoms of –SO₃Na on the surface of the ZnO/**PNSO₃Na** film, has been discovered. The strong high resolution peaks of Na 1s and S 2p in the ZnO/**PNSO₃Na** film further demonstrate that the hyperbranched SME, **PNSO₃Na**, has been successfully deposited on the surface of ZnO.

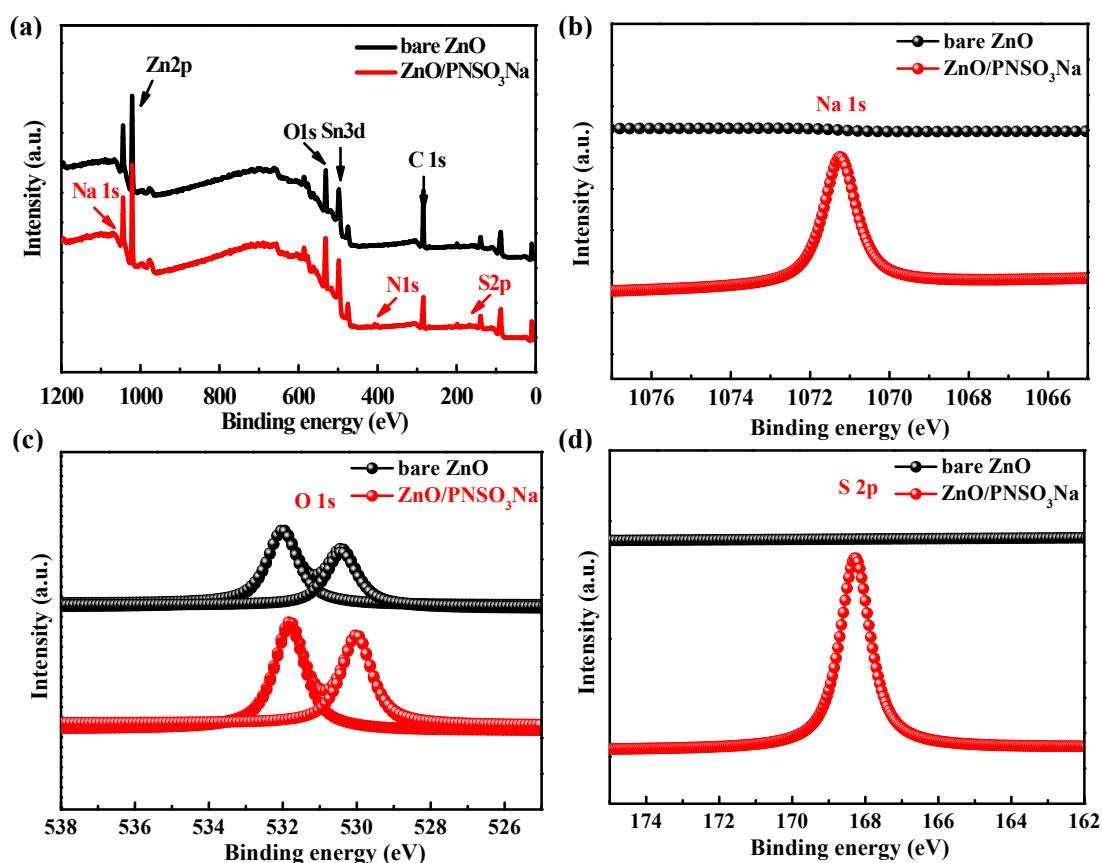


Fig. S2 (a) Survey X-ray photoelectron spectra (XPS) and high-resolution XPS of (b) Na 1s, (c) O 1s and (d) S 2p on the surface of ZnO and ZnO/**PNSO₃Na** ETLs spin-coated onto the ITO substrate.

The UV-vis absorption spectra of the ZnO and ZnO/PNSO₃Na films spin-coated on ITO have been measured, as described in Fig. S3a (ESI†). Obviously, due to the ultrathin film of PNSO₃Na, ZnO and ZnO/PNSO₃Na exhibit analogous optical absorption profiles with an absorption band onset (λ_{onset}) at ~ 380.37 nm. The optical transmittance spectra of ZnO and ZnO/PNSO₃Na have been characterized as depicted in Fig. S3b (ESI†). Both ZnO and ZnO/PNSO₃Na possess a high transparency of $>85\%$ between 360–800 nm, suggesting that introducing the hyperbranched SME would not hamper the optical absorption of the active layer.

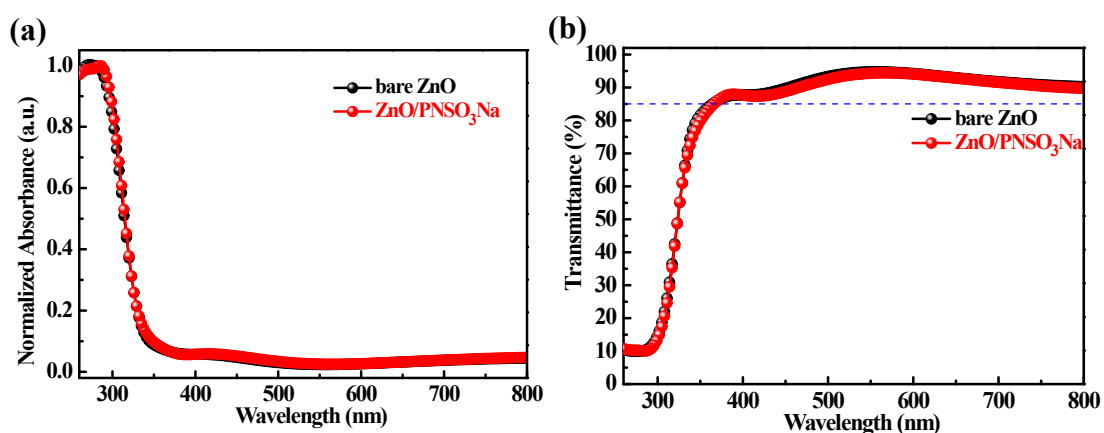


Fig. S3 (a) Normalized UV-vis absorption spectra and (b) optical transmittance spectra of ZnO and ZnO/PNSO₃Na films spin-coated on ITO.

From the UV–vis absorption and cyclic voltammogram (CV) spectra of **PNSO₃Na** film (Fig. S4, ESI†), the associated E_g^{opt} is 2.18 eV, which is associated with the E_g^{ec} of 2.09 eV from CV measurement. The associated HOMO and LUMO energy levels are -5.65 eV and -3.56 eV, respectively.

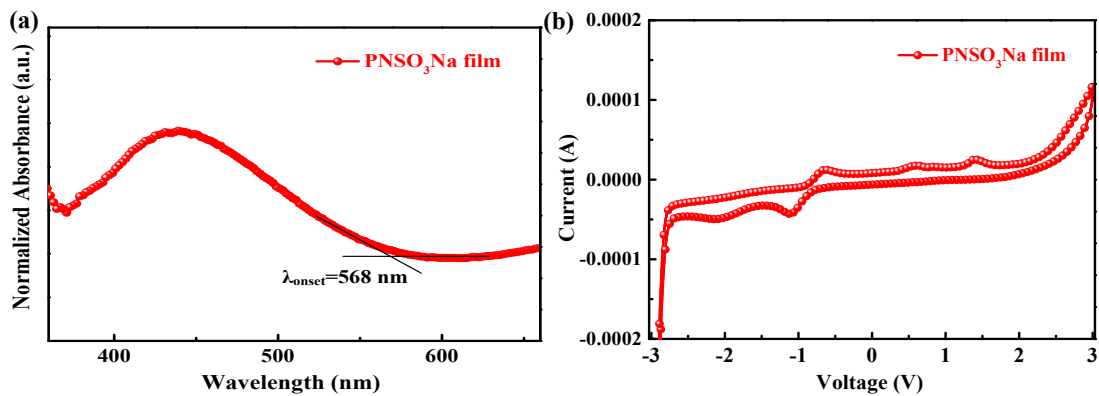


Fig. S4 (a) UV-visible absorption spectrum of hyperbranched small molecule electrolyte **PNSO₃Na** spin-coated on quartz plate. (b) Cyclic voltammogram of **PNSO₃Na** measured at a scan rate of 50 mV/S⁻¹, vs. Ag/Ag⁺ in a 0.1 M (C₄H₉)₄NPF₆ solution.

The high binding energy cutoffs (E_{cutoff}) of ZnO and ZnO/PNSO₃Na are 13.90 eV and 14.34 eV, respectively, and the associated binding energy onset (E_{onset}) located at 0.48 eV (ZnO) and 0.42 eV (ZnO/PNSO₃Na). The highest occupied molecular orbital (HOMO) energy levels of ZnO and ZnO/PNSO₃Na are 7.80 eV and 7.30 eV, respectively. Based on the HOMO energy levels and the $E_{\text{g}}^{\text{opt}}$ (3.26 eV) obtained from the above UV-vis absorption spectra (Fig. S3a, ESI[†]), the lowest unoccupied molecular orbital (LUMO) energy levels of ZnO and ZnO/PNSO₃Na are calculated to be -4.54 eV and -4.04 eV, respectively.

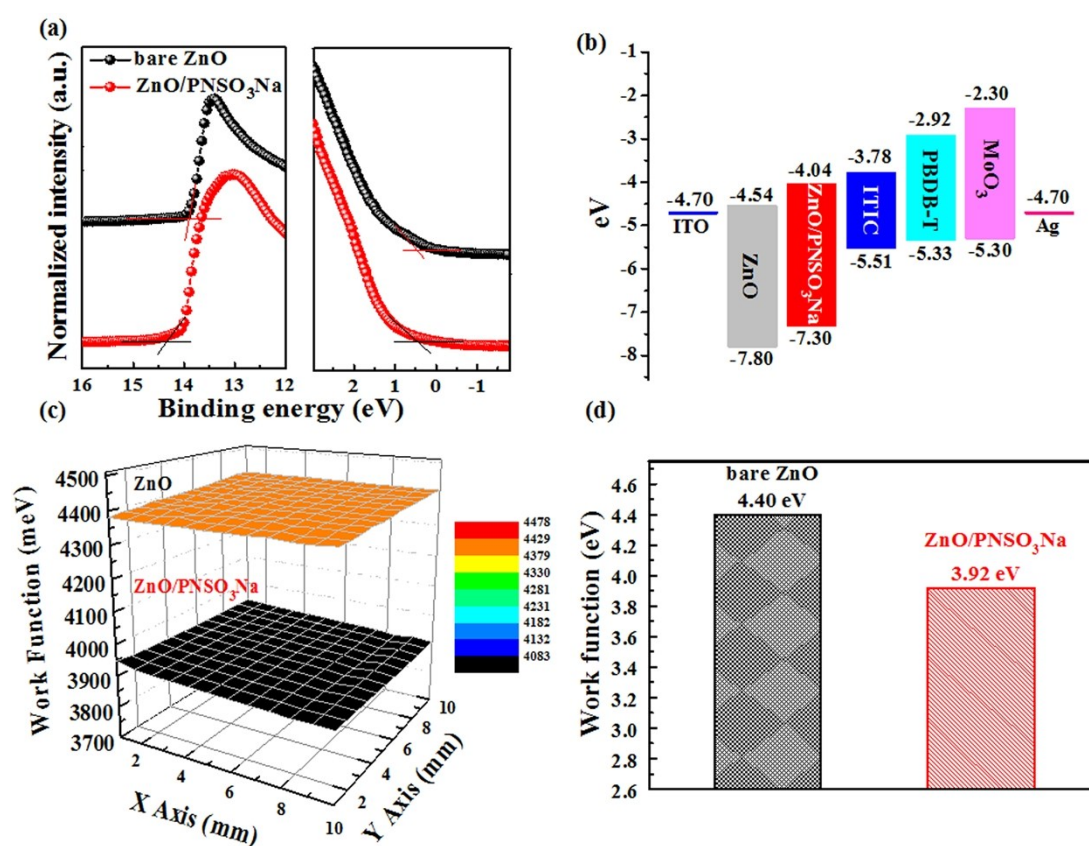
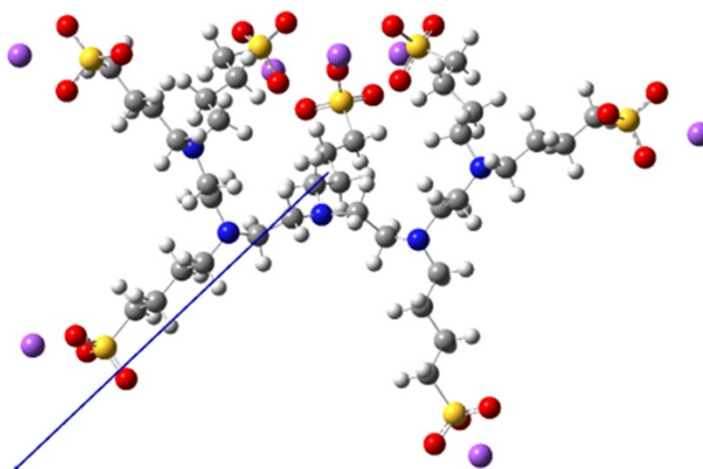


Fig. S5 (a) Ultraviolet photoelectron spectroscopy (UPS) spectra of (left) the inelastic cutoff region and (right) the HOMO region of bare ZnO and ZnO/PNSO₃Na ETLs. (b) Energy-level diagram of the PSCs and electrical contacts of the ETLs based on PBDB-T:ITIC device. (c) Work function images from Kelvin probe microscopy (KPM) matrix. (d) The schematic diagram of work function according to KPM.



The dipole moment is 8.2839 D

Fig. S6 The geometry of the ground state of the hyperbranched electrolyte of PNSO_3Na was optimized by density functional theory (DFT) at the B3LYP/6-31G** level with Gaussian-09 package. The dipole moment is 8.2839 D.

Table S1. Energy levels of the ZnO and ZnO/PNSO₃Na.

ETL	E_{cutoff} (eV)	E_{onset} (eV)	HOMO (eV)	HOMO (eV)	^aΔΦ (eV)	KPM (eV)
ZnO	13.90	0.48	-7.80	-4.54	-	4.40
ZnO/PNSO ₃ Na	14.34	0.42	-7.30	-4.04	-0.50	3.92

^aΔΦ are for the difference in the work function of ZnO and PNSO₃Na modified ZnO according to UPS, -HOMO = hv - (E_{cutoff} - E_{onset}), where hv = 21.22 eV.

Table S2. Photovoltaic performance of inverted PBDB-T:ITIC solar cells with bare ZnO and ZnO/PNSO₃Na ETLs.

Active Layer	ETL	V_{oc} (V)	J_{sc} (mA/cm ²)	FF (%)	PCE (%)
PBDB-T:ITIC	ZnO	0.861	17.815	64.7	9.9
PBDB-T:ITIC	ZnO/PNSO ₃ Na	0.874	18.658	68.7	11.2

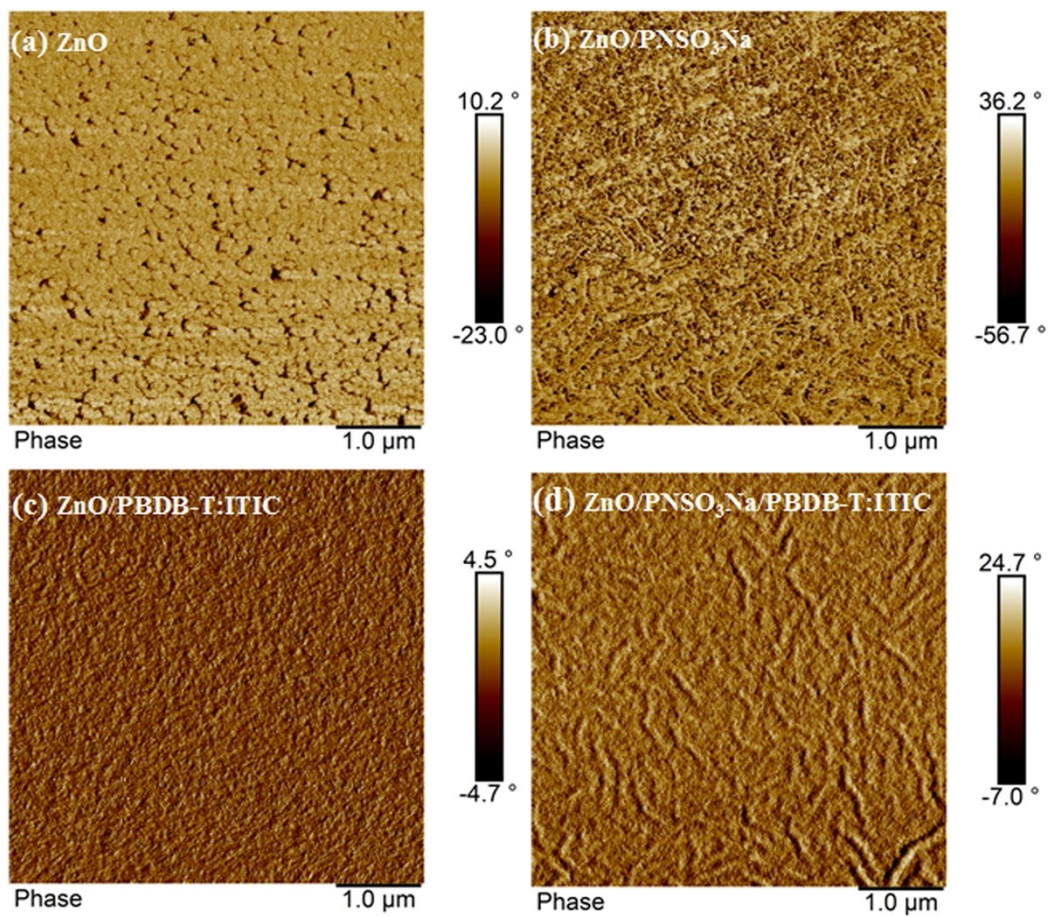


Fig. S7 Atomic force microscopy (AFM) phase image on the surface of (a) ZnO. (b) ZnO/PNSO₃Na. (c) ZnO/PBDB-T:ITIC. (d) ZnO/PNSO₃Na/PBDB-T:ITIC.

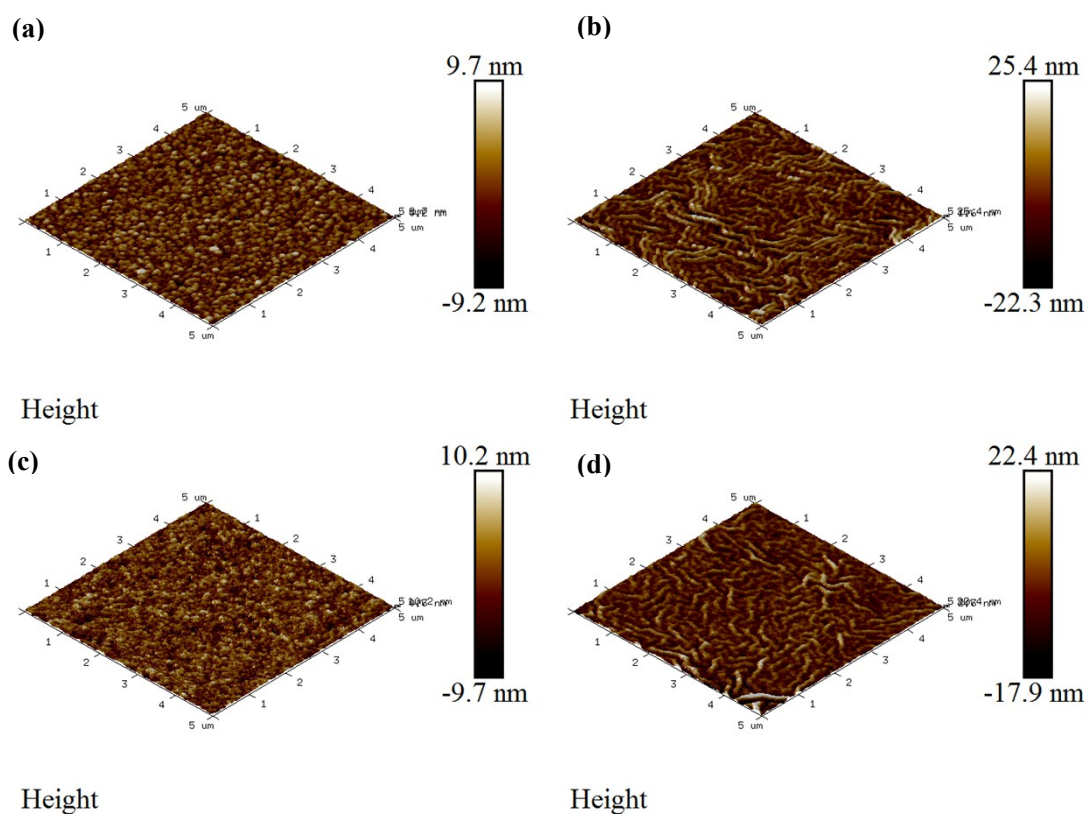


Fig. S8 Atomic force microscopy tapping mode three-dimensional image on the surfaces of (a) ZnO. (b) ZnO/PNSO₃Na. (c) ZnO/PBDB-T:ITIC and (d) ZnO/PNSO₃Na/PBDB-T:ITIC.

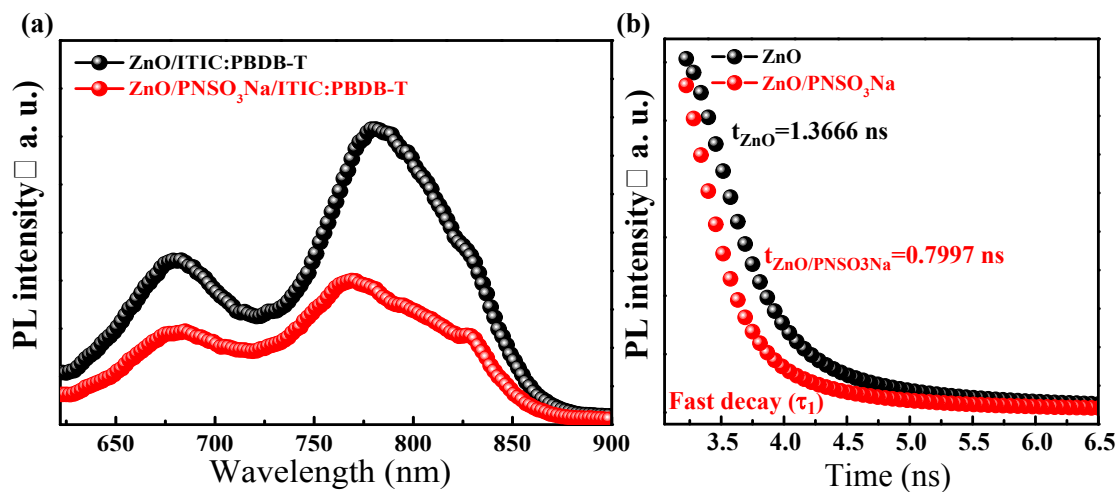


Fig. S9 (a) Steady-state photoluminescence spectra of PBDB-T-ITIC spin-coated on different ETL substrates excitation at 580 nm. (b) Time-resolved PL decay transients collected at 775 nm for all films in vacuum after excitation at 580 nm.

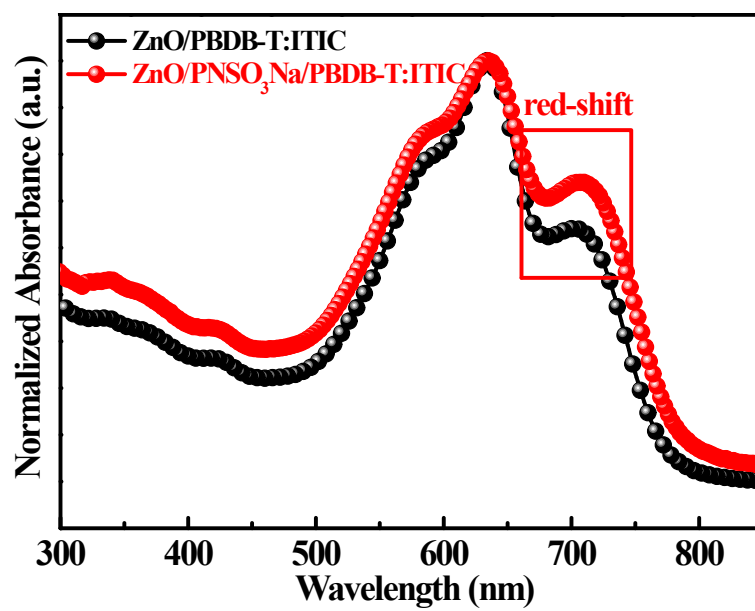


Fig. S10 Normalized UV-visible absorption spectra of the bare ZnO/PBDB-T:ITIC and ZnO/PNSO₃Na/PBDB-T:ITIC.

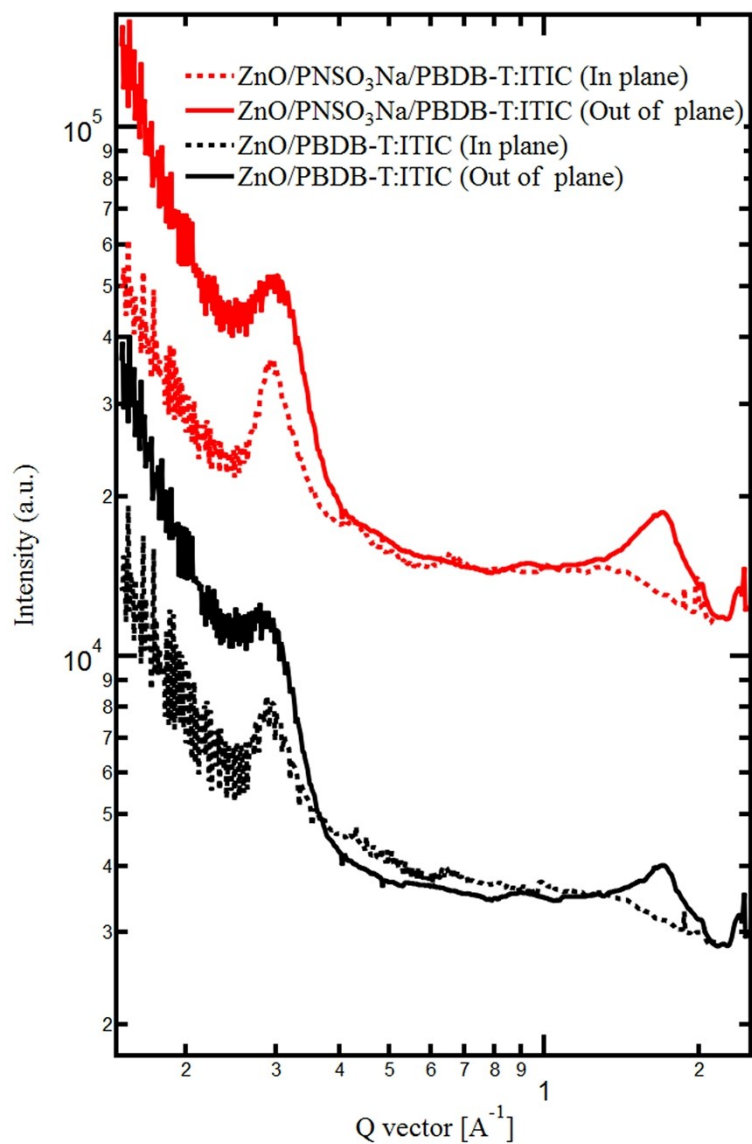


Fig. S11 Out-of-plane (solid lines) and in-plane (dash line) line-cut profiles of GIWAXS patterns of ZnO/PBDB-T:ITIC and ZnO/PNSO₃Na/PBDB-T:ITIC films.